

Research paper

Surface and structural studies in a PbCrO₄ Liesegang pattern with revert spacing

Dalia Ezzeddine, Houssam El-Rassy, Rabih Sultan

Department of Chemistry, American University of Beirut, P. O. Box 11-0236, Riad El Solh, 1107 2020 Beirut, Lebanon



HIGHLIGHTS

- EDX studies confirm the adsorption of CrO₄²⁻ on the precipitate.
- Isolated particles (observed under SEM) appear on the finer gel texture of the band bottom, and grow larger as the band number increases indicating an increasing extent of adsorption.
- AA measurements confirm the presence of more CrO₄²⁻ near the bottom of a band than in the remainder of a given interband region.

ABSTRACT

We present a novel study of a PbCrO₄ Liesegang pattern exhibiting revert spacing. Scanning Electron Microscopy (SEM), Atomic Absorption Spectrometry (AAS) and Energy Dispersive X-ray (EDX) spectroscopy measurements are carried out, and are shown to support the adsorption of CrO₄²⁻ on the precipitate, which becomes more enhanced as we move farther from the gel interface. Such an ascending differential adsorption scenario favors revert spacing over the direct spacing trend.

1. Introduction

The Liesegang experiment is known since 1896, when Raphael Eduard Liesegang discovered [1] Ag₂Cr₂O₇ rings separated by free space, as Ag⁺ and Cr₂O₇²⁻ interdiffuse in gel. In 1D space (such as a long tube), bands of precipitate and precipitate free domains form and alternate, as displayed in Fig. 1. In this reaction-diffusion system [2], the spacing between the bands increases as we go further away from the junction between the gel and the diffusing electrolyte (Fig. 1a and b). This observation, formulated by the Jablczynski spacing law [3], is a direct consequence of the coupling of the precipitation reaction to diffusion. The latter gradually retards the precipitate formation until the necessary nucleation threshold is attained, thus causing a band to form further away from the preceding one, and so on. This generally (but not universally) accepted mechanism is known as the Ostwald supersaturation-nucleation-depletion cycle [4]. Intriguingly, some experiments exhibit the opposing trend, wherein the inter-band spacing *decreases* with distance from the junction. This observation was coined *revert spacing* and occurs rather rarely, but reproducibly in some specific Liesegang systems. Liesegang experiments yielding revert spacing were reported notably in PbCrO₄ [5–9], Fe₃[Fe(CN)₆]₂ [10], AgI [11], AgBr [12], HgS [13], CuS [14] and CdS [15] precipitate systems.

The spacing law in a Liesegang pattern is expressed in either one of two essential forms:

Jablczynski's spacing law [3]:

$$\frac{x_{n+1}}{x_n} = 1 + p \quad (1)$$

Mathur's spacing law [11,18]:

$$x_n - x_{n-1} = a \left(\frac{s}{C_0 C'_0} \right)^{\alpha x_n} \quad (2)$$

where p in Eq. (1) is the so-called spacing coefficient, and n the band number; s in Eq. (2) is the solubility product, C_0 , and C'_0 the initial concentrations of the two ions, and a and α characteristic constants. Whereas in a direct (normal) spacing Liesegang pattern, the spacing coefficient p (Eq. (1)) is nearly constant, it typically decreases with band number in a revert pattern. In Mathur's law (Eq. (2)), the opposing situations of direct or revert pattern are represented by $\alpha > 0$ or $\alpha < 0$, respectively.

The study of Liesegang banding is extensive in the Physical Chemistry literature [2,16], due to its rich dynamical nature. Attention to revert spacing is rather scarce, but is gradually growing. Mathur and Ghosh [17,18] postulated that revert spacing is caused by the tendency of the diffusing electrolyte to peptize or dissolve out the precipitate. Flicker and Ross [10] proposed a mechanism of instability due to an autocatalytic particle growth from a homogeneous colloidal suspension. According to this mechanism, revert spacing arises when the diffusion

E-mail address: rsultan@aub.edu.lb (R. Sultan).

<https://doi.org/10.1016/j.cplett.2019.136735>

Received 27 July 2019; Received in revised form 29 August 2019; Accepted 1 September 2019

Available online 05 September 2019

0009-2614/ © 2019 Elsevier B.V. All rights reserved.

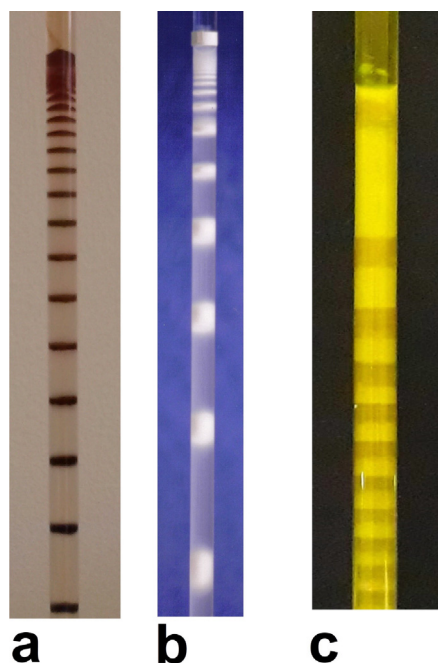


Fig. 1. Paradigms of Liesegang patterns involving different salt precipitates: (a) $\text{Ag}_2\text{Cr}_2\text{O}_7$; (b) $\text{Mg}(\text{OH})_2$; (c) PbCrO_4 . Whereas the first two follow the direct spacing trend, the third exhibits revert spacing.

coefficient and the concentration of the colloid sol decrease with increasing distance from the gel boundary. Other mechanisms based on post-nucleation patterning and the growth of particles from a colloid were advanced by Müller et al. [19,20]. Ramasamy et al. [5,15] developed the theory of preferential adsorption of the diffusing co-precipitate ion and tested it in PbCrO_4 and CdS systems. Prior to this work, the same group had introduced [11] a theory based on the DLVO theory of the stability of colloids, to explain revert spacing and the transition from revert to normal spacing in an AgI Liesegang pattern. The theory essentially considers the charge on the sol particles, and the reversal of this charge across the zero point. The formation of the PbCrO_4 pattern is light sensitive. The bands do not form in the dark [7] and achieve a much better morphology when exposed to sunlight. In a recent work by Kulkarni et al. [12], revert spacing in an AgBr Liesegang pattern (Br^- in the gel, Ag^+ diffusing) was attributed to the peptization of the sol particles, which was shown to decrease as the concentration of diffusing Ag^+ decreases. Based on an elaborate DLVO model, they argued that the Ag^+ ion number density after each band formation should correspond to a critical coagulation concentration.

In a previous work [8], we investigated the revert spacing phenomenon in a PbCrO_4 Liesegang pattern (Fig. 1c), formed from a K_2CrO_4 solution diffusing into a $\text{Pb}(\text{NO}_3)_2$ -agar gel. The morphological

characteristics of the revert pattern were studied and contrasted with a CuCrO_4 Liesegang pattern exhibiting direct spacing. The amount of adsorbed chromate ions on the successive bands of the pattern was estimated by UV spectrophotometry. In the present paper, we carry out structural investigations by employing techniques such as Scanning Electron Microscopy (SEM), Atomic Absorption Spectrometry (AAS) and Energy Dispersive X-ray (EDX) spectroscopy to further test the role of adsorption in architecting the revert pattern.

2. Experimental

2.1. Preparation of the pattern

A sample of $\text{Pb}(\text{NO}_3)_2$ (Fluka, 99.0%; of mass 0.0165 g), was dissolved in 50.00 mL of double distilled water with the desired amount of agar powder (Bacto agar, with minimum extraneous matter, pigmented portions and salts), to make 0.0010 M $\text{Pb}(\text{NO}_3)_2$ in 1.0% w/w gel. The mixture was heated to 85°C under constant stirring until a homogeneous solution was obtained. The resulting solution was then poured into a set of 1D Pyrex tubes of 1.0 cm diameter and 24.0 cm length, filling each to two-thirds. The solution was left to gel for six hours at room temperature. Then a solution of the outer electrolyte (K_2CrO_4 ; Fluka, 99.0%) of concentration 0.20 M was gently poured on top of the lead nitrate-doped gel. The tubes were then covered with parafilm and exposed to sunlight for at least two weeks at room temperature.

2.2. Analysis

After cutting the tube, the gel was taken out gently, via a perfect sliding operation. The bands and the interband regions were then carefully separated by meticulous cutting for structural, compositional, and morphological characterization. Scanning electron microscopy (SEM) was performed using a MIRA3 Tescan electron microscope after coating the samples with a thin layer of gold (15 nm thickness). Atomic Absorption Spectrometry (AAS) was conducted on a SOLAAR atomic absorption spectrophotometer equipped with an ASX-510 autosampler and a G95 graphite furnace.

3. Results and discussion

3.1. SEM studies

The general appearance of the pattern is displayed in Fig. 1c. We clearly notice the decrease in spacing between the PbCrO_4 bands as they move away from the junction. The phenomenology of the pattern and its characteristics was analyzed in previous studies [8,9]. The increase in the fraction of adsorbed CrO_4^{2-} ions on the bands as the band order (number) increases was demonstrated by spectrophotometric analysis. We now investigate the structural features of the bands. Fig. 2 shows micrographs of the bottom of the first three bands (labeled 1, 2 and 3

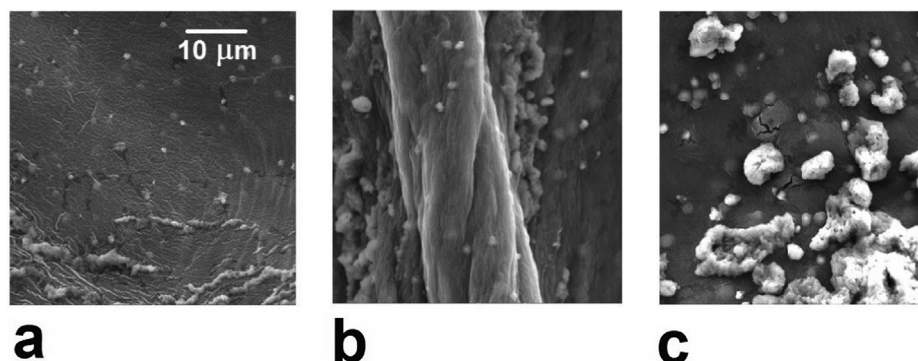


Fig. 2. Scanning electron micrographs for a PbCrO_4 Liesegang pattern exhibiting revert spacing. (a) band 1; (b) band 2; (c) band 3.

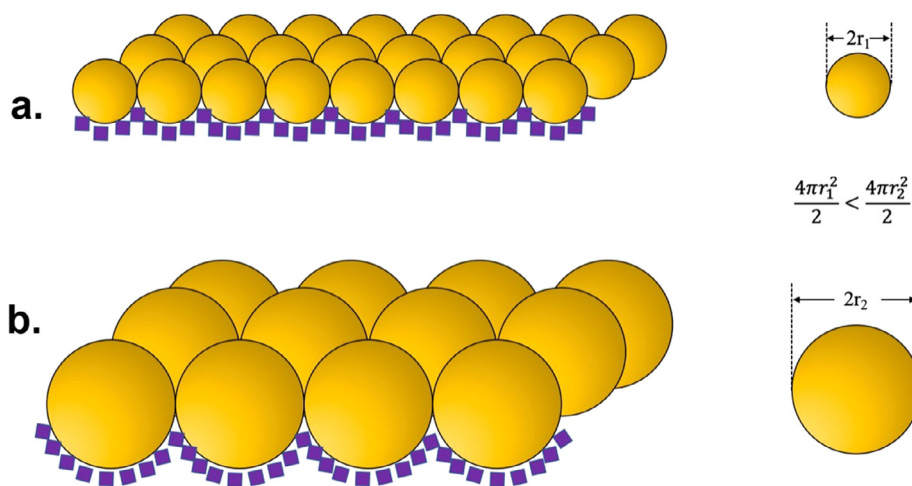


Fig. 3. Illustrative graphic of the bottom surface of a band at the top of the pattern (a), and the bottom of the pattern (b). The particles at the bottom (spheres) are fewer and larger in congruence with Ostwald ripening. Although with fewer particles at the bottom, the number of adsorbed CrO_4^{2-} (small squares) is larger because of the greater surface area.

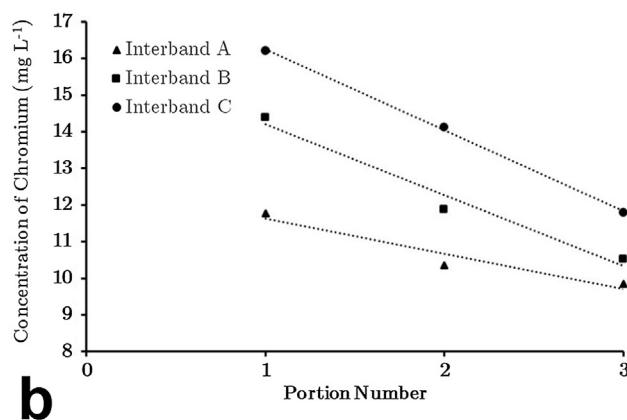
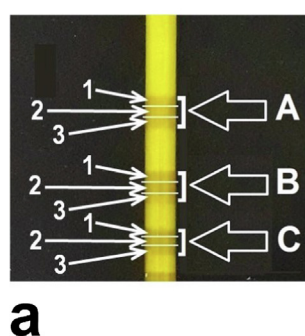
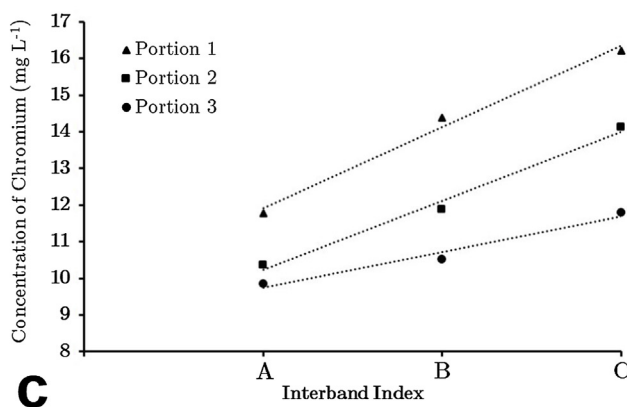
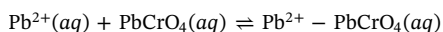


Fig. 4. Atomic absorption analysis of the interband gel regions A, B and C. (a) A display of the analyzed regions. The spacings A, B and C are 0.80, 0.70 and 0.55 cm respectively. Each region is divided into three equal portions (1, 2 and 3), each analyzed separately. (b) Variation of Cr content with gel portion within the same interband. The three curves correspond to interband regions A (\blacktriangle), B (\blacksquare) and C (\bullet) described in frame a. (c) Variation of Cr content with interband order (A, B, and C) for the same gel portion number. The three curves correspond to portions 1 (\blacktriangle), 2 (\blacksquare) and 3 (\bullet). The relative standard deviation is $< 1\%$.



respectively). Within the embedded texture, we observe distinct isolated particles whose size notably increases as we go from band 1 to 2 to 3. We attribute those particles to the adsorbed CrO_4^{2-} on the PbCrO_4 precipitate. In Ref. [9], the lead ions in the interband region were shown to be distributed between free Pb^{2+} and the complex $\text{Pb}^{2+}\text{-PbCrO}_4$, according to the established equilibrium:



The $\text{Pb}^{2+}\text{-PbCrO}_4$ complex was characterized by mass spectrometry [9]. The free Pb^{2+} are thus coulombically attracted by the adsorbed CrO_4^{2-} and precipitated as those particles appearing in Fig. 2. Similarly,

the positively charged complex ions are attracted closer to the first band. When more CrO_4^{2-} diffuse, they displace the Pb^{2+} from the complex, precipitating the second band, and so on. The eminent feature here is that the second band forms closer to the former one than in a normal Liesegang pattern because of the said attraction. This mechanism is further supported by the striking observation that Pb^{2+} is completely absent from the interband aqueous region, analyzed by AAS after elimination of the gel.

It is to be further noted that the particle size also increases as we move away from the junction point, in congruence with the phenomenon of Ostwald ripening [21–24]. Although this might seemingly

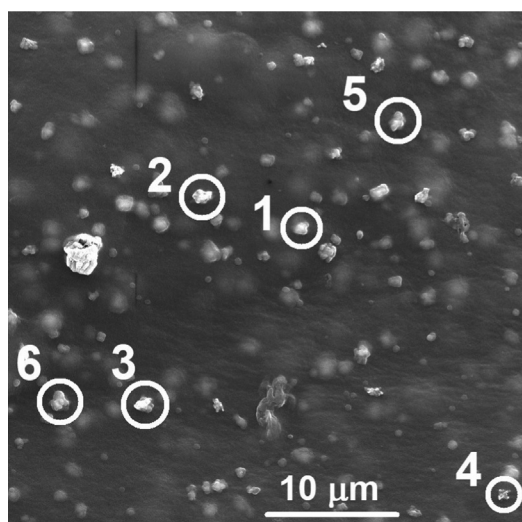


Fig. 5. Bottom of band No. 2 with selected particles 1–6. Each numbered particle is analyzed separately by EDX spectroscopy for the negative/positive charge ratio. The results are recorded in Table 1.

Table 1

EDX analysis of particles 1–6 shown in Fig. 5. The last column reports the % remaining Cr ($\times 2$)/%K after neutralization by Pb^{2+} .

Region	% Pb	%Cr	%K	$\ominus/\oplus(\text{Cr}/\text{K})$
1	1.55	8.34	14.08	0.96
2	2.11	8.03	12.12	0.98
3	2.42	7.53	10.00	1.02
4	0.91	8.04	13.37	1.07
5	1.14	8.94	12.84	1.21
6	2.52	8.58	10.91	1.11

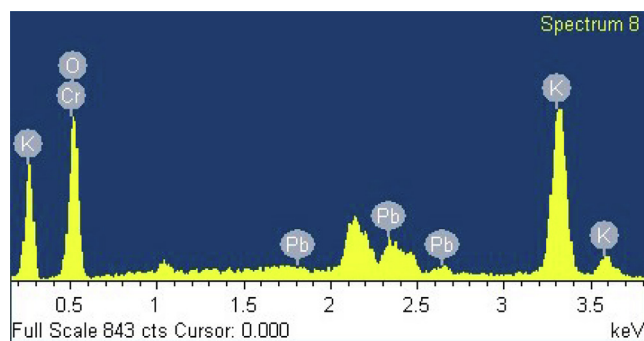


Fig. 6. EDX spectrum of the particle in region 5 of Figure 5. From Table 1, the atomic percentages of Pb, Cr and K are 1.14, 8.94 and 12.84 respectively. The present chromate ions (CrO_4^{2-}) neutralized by Pb^{2+} is 1.14. This leaves 7.80% chromate. The potassium percent necessary to neutralize the remaining chromate ions = $7.80 \times 2 = 15.6$. Since only 12.84 K is present in the particle, there remains 2.56% excess negatively charged chromate. The ratio of $\text{CrO}_4^{2-} (-) \text{K}^+ (+)$ is thus 1.21, which appears in the last column of Table 1.

decrease the adsorption at later bands due to fewer particles, we believe the surface area prone to adsorption remains larger because it is facilitated by the bigger size. This argument is illustrated in Fig. 3.

3.2. AAS studies

Measurement of the chromium concentration in the interband regions was performed by Atomic Absorption Spectrometry (AAS), after dividing each interband region into three equal portions: an upper (portion 1), a central (portion 2), and a lower one (portion 3), as

depicted in Fig. 4a. The number of interbands investigated separately in this study is limited to three, since it was not possible to accurately isolate the interbands beyond the third due to their closeness to each other and their narrowness. It is important to note here that the present analysis is carried out after a long time (three weeks), and hence the concentration differences cannot be attributed to the on-going diffusion process.

The data consistently shows a decrease in chromium concentration within each interband taken separately, wherein the highest concentrations were detected in the portion closest to the previous band. It is worth mentioning that the measured concentrations average the mass density of chromium within each isolated portion from the explored interband regions. A plot of the chromium concentration within each interband region separately (over portions 1–3), reveals a linear decrease with a negative slope as we go farther away from the band bottom. This confirms the previously reported mechanism [8], establishing that the high chromate concentration near the band bottom is due to CrO_4^{2-} adsorption on the precipitate. Fig. 4b shows the described decrease for three distinct interband regions. The concentration gradient found herein within each interband supports experimentally the presence of more chromate ions available next to the bottom of the previous band. Based on this, it was previously argued [8] that the adsorption of chromate ions on that band attracts the lead ions (Pb^{2+}), and hence causes the nucleation of the next band to take place closer to the previous band than in the normal trend. This mechanism was demonstrated [8] based on the measurement of the fraction of adsorbed chromate on the consecutive bands by UV spectrophotometry. We now verify the adsorption trend over consecutive interband regions. Fig. 4c displays a plot of $[\text{Cr}]$ for each portion separately (first, second and third portions between the two distinct separating lines) as we go from interband A to B to C. We clearly note an increase in $[\text{Cr}]$ for a given portion number with interband index (A, B and C respectively). The correlation is further confirmed by observing that the slope of the line is highest for portion 1 and lowest for portion 3, in a decisive support of the role of increasing adsorptivity. This also shows that the evolution of a specific band continues during and after the appearance of its succeeding band, since the chromium concentration per portion within a region and as an average for the whole interband region, increases linearly as we go further down. Last but not least, we also recall that the effect of increasing adsorptivity of CrO_4^{2-} with band number observed in this revert pattern exactly opposes the (decreasing) adsorption trend in a CuCrO_4 Liesegang pattern exhibiting direct spacing [8].

3.3. EDX studies

We further perform SEM-EDX¹ measurements on selected regions from the bottom of a selected band. We choose the bottom of the second band whose representative scanning electron micrograph is displayed in Fig. 5.

We analyze the EDX spectrum in randomly distributed particles (18 regions overall). In Table 1, we report the results for particles labeled 1 to 6 in Fig. 5. The results are recorded in Table 1.

The EDX data reveal that for most (12 out of 18 $\equiv 66.7\%$) of the particles analyzed (selected randomly), the particle has an excess negative charge, thus favoring the attraction of the Pb^{2+} in the gel, during the dynamical diffusion process. Potassium ions (K^+) do appear in the particle, but they most of the time do not exceed the charge necessary to neutralize the adsorbed chromate ions, hence keeping the particle overwhelmingly negative. A sample analysis of the EDX spectrum for an adsorbed particle on the surface (region 5 in Table 1), is explained in the caption of Fig. 6.

This is a clear confirmation of the presence of negatively charged adsorbed CrO_4^{2-} on the PbCrO_4 precipitate particles present on the

¹ Energy Dispersive X-ray spectroscopy.

bottom of the bands.

4. Conclusions

This study provides evidence for the role of adsorption of CrO_4^{2-} ions on the formed PbCrO_4 precipitate bands in mediating the revert spacing in this PbCrO_4 Liesegang system. The adsorption, which takes place in an ascending trend, is established to be responsible for the formation of the precipitate bands closer to their predecessors than usual. This obviously leads to the revert spacing situation. It is worth noting that in some previous studies [17,12], the empirical spacing law in revert systems was based on the calculation of a flocculation or coagulation threshold Γ , which decreases with band number. This formulation was later augmented by the theory of preferential adsorption of the ions of the diffusing co-precipitate [11]. The findings in the present study may be summarized as follows:

1. Isolated particles (observed under SEM) appear on the finer gel texture of the band bottom, due to the attraction of some free and complexed Pb^{2+} ions, and their delayed precipitation as PbCrO_4 . Those particles grow larger as the band number increases due to increasing extent of adsorption.
2. AAS measurements at late times rigorously confirm the presence of more CrO_4^{2-} near the bottom of a band than in the remainder of a given interband region.
3. EDX measurements reveal that the \ominus/\oplus ratio inside selected PbCrO_4 particles of delayed formation is dominantly greater than 1, in a clear indication of the presence of negatively charged adsorbed CrO_4^{2-} on the precipitate.

Acknowledgement

This work was supported by a grant from the Lebanese National Council for Scientific Research (LNCSR). All the AA, SEM and EDX measurements were performed in the Central Research Science Lab (CRSL), American University of Beirut.

References

- [1] R.E. Liesegang, Über Einige Eigenschaften von Gallerten, Naturw. Wochenschr. 11 (1896) 353–362.
- [2] H.K. Henisch, Crystals in Gels and Liesegang Rings, Cambridge University Press, Cambridge, 1988.
- [3] C.K. Jablczynski, Mémoires Présentés à la Société Chimique. Les Anneaux de Liesegang, Bull. Soc. Chim. France 33 (1923) 1592–1602.
- [4] W. Ostwald, Lehrbuch der Allgemeinen Chemie, 2. Aufl., Band II, 2. Teil: Verwandtschaftslehre, Engelmann, Leipzig, 1899, p. 779.
- [5] N. Kanniah, F.D. Gnanam, P.A. Ramasamy, New spacing law for Liesegang rings, Proc. Indian Acad. Sci. (Chem. Sci.) 93 (1984) 801–811.
- [6] I. Das, A. Pushkarna, R.S. Lall, Light induced periodic precipitation and crystal growth of PbCrO_4 . A novel study in two-dimensional gel media, J. Cryst. Growth 82 (1987) 361–366.
- [7] I. Das, A. Pushkarna, Light induced periodic precipitation and chemical instability in lead chromate systems, J. Non-Equil. Thermodyn. 13 (1988) 209–220.
- [8] T. Karam, H. El-Rassy, R. Sultan, Mechanism of revert spacing in a PbCrO_4 Liesegang System, J. Phys. Chem. A 115 (2011) 2994–2998.
- [9] L. Kalash, H. Farah, A. Zein Eddin, R. Sultan, Dynamical profiles of the reactive components in direct and revert Liesegang patterns, Chem. Phys. Lett. 590 (2013) 69–73.
- [10] M. Flicker, J. Ross, Mechanism of chemical instability for periodic precipitation, J. Chem. Phys. 60 (1974) 3458–3465.
- [11] N. Kanniah, F.D. Gnanam, P. Ramasamy, G.S. Laddha, Revert and direct type Liesegang phenomenon of silver iodide: factors influencing the transition point, J. Colloid Interf. Sci. 80 (1981) 369–376.
- [12] S.D. Kulkarni, P.C. Walimbe, R.B. Ingulkar, J.D. Lahase, P.S. Kulkarni, Revert banding in one-dimensional periodic precipitation of the ($\text{AgNO}_3 + \text{KBr}$) system, ACS Omega 4 (2019) 13601–13608.
- [13] B.M. Mehta, K. Kant, Periodic precipitation of mercury sulphide, Kolloid-Z.u.Z.Polymer 209 (1966) 58–60.
- [14] B.M. Mehta, K. Kant, Formation of Liesegang rings of copper sulphide, Kolloid-Z.u.Z.Polymer 209 (1966) 54–56.
- [15] N. Palaniandavar, F.D. Gnanam, P. Ramasamy, Diffusion controlled autocatalytic growth of revert periodic precipitation of cadmium sulphide in lyophilic colloid, J. Chem. Phys. 80 (1984) 3446–3450.
- [16] K. Stern, The Liesegang phenomenon, Chem Rev. 54 (1954) 79–99.
- [17] P.B. Mathur, S. Ghosh, Liesegang rings. Part I. Revert system of Liesegang rings, Kolloid-Zeitschrift Und Zeitschrift Für Polymere 159 (1957) 143–146.
- [18] M.P. Behari, Structural analysis of Liesegang ring systems, Bull. Chem. Soc. Japan 34 (1961) 440–442.
- [19] D.S. Chernavskii, A.A. Polezhaev, S.C. Müller, A model of pattern formation by precipitation, Physica D 54 (1991) 160–170.
- [20] S.C. Müller, A.A. Polezhaev, Complexity of precipitation patterns: comparison of simulation with experiment, Chaos 4 (1994) 631–636.
- [21] W. Ostwald, Über die Vermeintliche Isomerie des Roten und Gelben Quecksilberoxyds und die Oberflächenspannung Fester Körper, Z. Phys. Chem. 34 (1900) 495.
- [22] R.E. Liesegang, Über die Reifung von Silberhalogenidemulsionen, Z. Phys. Chem. (Leipzig) 75 (1911) 374–377.
- [23] I. Lifshitz, V.V. Slyozov, The kinetics of precipitation from supersaturated solutions, J. Phys. Chem. Solids 19 (1961) 35.
- [24] L. Ratke, P.W. Voorhees, Growth and Coarsening, Ostwald Ripening in Material Processing, Springer, Berlin, 2002.